

See discussions, stats, and author profiles for this publication at: <https://www.researchgate.net/publication/259875085>

# A New System for Studying Spatial Front Instabilities: The Supercatalytic Chlorite–Trithionate Reaction

ARTICLE *in* THE JOURNAL OF PHYSICAL CHEMISTRY A · JANUARY 2014

Impact Factor: 2.69 · DOI: 10.1021/jp410470r · Source: PubMed

CITATION

1

READS

24

5 AUTHORS, INCLUDING:



**Csekő György**

China University of Mining Technology

15 PUBLICATIONS 66 CITATIONS

SEE PROFILE



**Qingyu Gao**

China University of Mining Technology

86 PUBLICATIONS 423 CITATIONS

SEE PROFILE



**Attila K Horváth**

University of Pécs

54 PUBLICATIONS 536 CITATIONS

SEE PROFILE

# A New System for Studying Spatial Front Instabilities: The Supercatalytic Chlorite–Trithionate Reaction

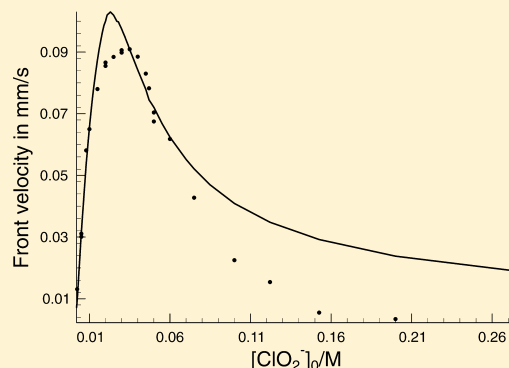
György Csekő,<sup>†,‡</sup> Lin Ren,<sup>§</sup> Yang Liu,<sup>§</sup> Qingyu Gao,<sup>\*,§</sup> and Attila K. Horváth<sup>\*,†,‡</sup>

<sup>†</sup>Department of Inorganic Chemistry, University of Pécs, Ifjúság útja 6., H-7624 Pécs, Hungary

<sup>‡</sup>János Szentágothai Research Center, Ifjúság útja 20., H-7624 Pécs, Hungary

<sup>§</sup>College of Chemical Engineering, China University of Mining and Technology, Xuzhou 221116, People's Republic of China

**ABSTRACT:** We show that the chlorite–trithionate reaction is “supercatalytic”; i.e., the formal kinetic order of the autocatalyst  $\text{H}^+$  is 2. A simple model is proposed and discussed to describe the unusual concentration dependencies of one-dimensional front propagation found experimentally. It is also demonstrated that at relatively wide concentration ranges the linear two-dimensional front initiated loses its stability, giving rise to an appearance of cellular structures in a convection-free system. Compared to the chlorite–tetrathionate reaction, however, this system is much more stable at alkaline conditions, even for hours; therefore, no side reactions can be taken into consideration to check whether they may have any side effects on the evolution of spatiotemporal structures.



## INTRODUCTION

The chlorite–tetrathionate (CT) reaction has been playing a substantial role for studying several nonlinear phenomena in connection with front propagation such as pattern formation,<sup>1</sup> 2D- and 3D-front instabilities<sup>2–7</sup> and spatial bistability<sup>8,9</sup> for almost two decades. An earlier study indicated that a simplified model including a simple rate equation combined with the thermodynamically most favorable stoichiometry<sup>10</sup> describes all the experimentally observable phenomena qualitatively well within a narrow concentration range of the reactants. This model is being used exclusively despite the facts that several concerns have already been enlightened about the uncertainty in stoichiometry<sup>11</sup> and in rate coefficients being used to simulate the experimental results.<sup>8,10</sup> Recently it has also been demonstrated<sup>12</sup> that the most serious problem with this system is the alkaline decomposition of tetrathionate<sup>13–16</sup> resulting in the formation of thiosulfate, trithionate, and sulfite. Thus, when sodium hydroxide is used for stabilizing the reacting system prior to initiation, especially at higher hydroxide concentrations, the alkaline decomposition of tetrathionate may be completed within approximately half an hour, meaning that the composition of chlorite–trithionate, chlorite–thiosulfate, and chlorite–sulfite reactions is studied instead of the original CT system. It is, therefore, an eager expectation to find another system that first shows “supercatalysis” (i.e., the formal kinetic order of  $\text{H}^+$  that acts as an autocatalyst is at least 2), and second, has the reactants that may spend significant time together at alkaline conditions without any primary decomposition or reaction. It is well-known that trithionate is much more stable in alkaline conditions than other polythionates<sup>17,18</sup> excluding dithionate; therefore, the chlorite–trithionate reaction seems to be a good candidate to fulfill all the criteria

mentioned above. In this paper we report on the preliminary results of kinetics of the chlorite–trithionate reaction along with the most important observations and explanations in the convection free 1D and 2D front propagation studies. We also provide a simple, but reasonable, model to study and simulate 1D or 2D front propagations.

## EXPERIMENTAL SECTION

**Materials.** Sodium trithionate was prepared as described previously,<sup>19</sup> and its purity was found to be better than 99.5%. Commercially available sodium chlorite was recrystallized twice from an ethanol–water mixture and its purity was found to be better than 99% by iodometric titrations. Stock solutions were freshly prepared each day from double-distilled and twice ion-exchanged water. The pH of solutions in the case of kinetic studies was regulated between 4.25 and 5.15 by acetic acid/acetate buffer taking the  $\text{pK}_a$  of acetic acid as 4.55. The acetate concentration was kept constant at 0.167 M, and the pH was adjusted by the necessary amount of acetic acid. The ionic strength was adjusted at 0.5 M by addition of the necessary amount of sodium perchlorate solution. Some control experiments were also carried out at 1.5 M ionic strength with varying concentrations of the buffer components. The temperature was maintained at  $25.0 \pm 0.1$  °C at each kinetic run. Concentrations of trithionate and chlorite ion were varied between 0.57–31.7 and 0.39–15.7 mM, respectively. In this experimental setup we investigated the reaction at 120 different experimental conditions and we also repeated our kinetic experiments at

Received: October 23, 2013

Revised: January 17, 2014

Published: January 22, 2014



several different cases that convinced us about good reproducibility of the kinetic curves.

For 1D-front experimental studies the concentrations of trithionate, chlorite, and hydroxide ion were varied among 1.0–20.0, 2.4–60.0, and 1.0–20.0 mM, respectively. Reactants were premixed in a known concentration of sodium hydroxide solution to prevent spontaneous initiation of front propagation. The front propagating was made to be visible by an addition of bromophenol blue acid–base indicator (0.0597 mmol/dm<sup>3</sup>). The chemical fronts were initiated by making a contact between a drop of 0.1 M hydrochloric acid solution and the reacting solution at one of the ends of the capillary tube. The capillary tube was then positioned and fixed horizontally. All these experiments were carried out at room temperature  $25 \pm 1$  °C.

Thin layer hydrogel of 0.6% agarose with an appropriate amount of reactants was utilized to investigate the two-dimensional front. Agarose solution was first prepared as described elsewhere,<sup>20</sup> by dissolving agarose in water at 100 °C and cooling to 35 °C. Then solutions of reagents and congo red indicator in necessary amounts were added and stirred vigorously. The mixture solution was gelatinized in a Plexiglas mold of 15 cm × 10 cm × 1 mm by cooling to 20 °C.

**Methods.** The kinetic experiments were followed by a Zeiss S10 diode array spectrophotometer. The reaction was carried out in a standard quartz cuvette equipped with a magnetic stirrer and Teflon cap having 1 cm optical path. The spectra of the reacting solutions in the wavelength range of 270–600 nm were acquired up to the end of the reaction (at least 90% conversion) but not for more than 40 000 s. The initial rate of the reaction was calculated from the absorbance–time series at 360 nm, where only chlorine dioxide absorbs ( $\epsilon = 1180 \text{ M}^{-1} \text{ cm}^{-1}$ ) and at 270 or 290 nm where the major absorbing species is chlorite ion ( $\epsilon = 126.0$  and  $93.7 \text{ M}^{-1} \text{ cm}^{-1}$ , respectively).

1D-front propagation studies were executed in a thin 50 cm long capillary tube having an inner diameter of  $0.733 \pm 0.006$  mm. After initiation, the position of reaction front was registered manually at regular time intervals. The front was allowed to propagate at least 30 cm. Except for the first 1–2 cm, a perfect linear relationship was found between the distance and time, meaning that the chemical front propagated with constant velocity.

For 2D-front propagation studies the chemical front was initiated by placing a filter paper strip containing the product mixture to one of the edges of gel soaked with the reactant solution. The gel was then covered with glass plate to prevent evaporation during the propagation and then transferred into a biochemical incubator for nitrogen protection at  $20 \pm 2$  °C. Evolution of the reaction-diffusion front was monitored using a CCD video camera (Tucsen, TCC–3.3ICE). Images were captured at every 60 s.

## CALCULATIONS

In the case of a one-dimensional reaction-diffusion front, the concentration of the  $i$ th species changes along the tube ( $x$ ) and with time ( $t$ ) denoted by  $c_i(x,t)$  is obtained by the partial differential equation

$$\frac{\partial c_i(x,t)}{\partial t} = D_i \frac{\partial^2 c_i(x,t)}{\partial x^2} + \sum_{j=1}^n S_{ij} r_j \quad (1)$$

where  $D_i$  is the diffusion coefficient of the  $i$ th species,  $S_{ij}$  is the stoichiometric number of the  $i$ th species in the  $j$ th reaction step,  $r_j$  is the rate of the  $j$ th reaction, and  $n$  is the number of reaction

steps in the model. If this is known for all species, the given partial differential equation system can be integrated with known initial concentrations and boundary conditions to obtain any  $c_i(x,t)$  values.

The partial differential equation system was numerically integrated using the second-order implicit backward differentiation formula<sup>21</sup> (BDF2 method) on a 2 cm long, one-dimensional tube and utilizing three-point-difference approximations for the 1D Laplacian operators. No-flux boundary conditions were applied at both ends of the tube. We divided the tube into 20001 grid cells (corresponds to  $h = 0.0001$  cm cell size). The initial concentrations in the first 1000 and the rest of the cells were set to the composition of the products solution and that of the unreacted mixture, respectively.

The position of the front was identified with  $[\text{H}^+] = 8 \times 10^{-5}$  M and the front velocity was calculated from the slope of the straight line fitted on the  $x_f$ – $t$  data usually in the 0.3–1.95 cm range. The correlation was always found to be perfectly linear.

## RESULTS AND DISCUSSION

**Stoichiometry.** Figure 1 shows typical kinetic runs at different initial conditions, indicating that chlorine dioxide

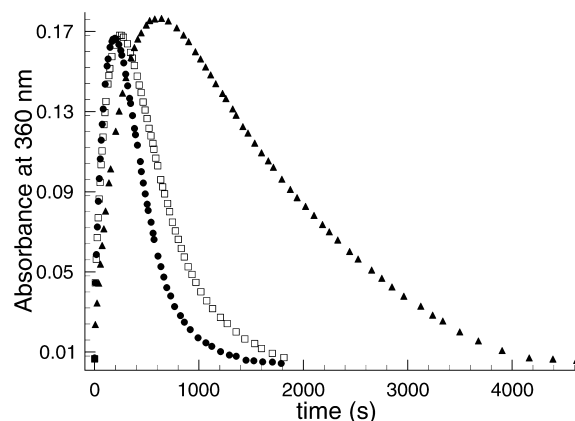


**Figure 1.** Experimental absorbance–time series in an excess of trithionate. Conditions are as follows:  $[\text{ClO}_2^-]_0 = 3.93$  mM, pH = 4.85.  $[\text{S}_3\text{O}_6^{2-}]_0/\text{mM} = 7.94$  ( $\blacktriangle$ ), 19.8 ( $\square$ ), and 27.8 ( $\bullet$ ).

forms during the course of reaction with no delay even in relatively high trithionate excess. Because it is already known that chlorine dioxide is capable of oxidizing trithionate as well,<sup>22</sup> the overall stoichiometry of the chlorite–trithionate reaction is also expected to be a complex one. In an excess of chlorite, where chlorine dioxide is an end product, the stoichiometric ratio (SR) defined as the ratio of the consumed chlorite over consumed trithionate concentrations can easily be determined in the following way. From the visible range one can easily determine the final concentration of chlorine dioxide (the only absorbing species at this wavelength range) from which its absorbance contribution to the final absorbance measured at the UV range can be calculated. Subtracting the absorbance (the remaining products do not absorb the light above 270 nm) obtained in this way from the measured ones one can easily determine the final concentration of chlorite; thus the SR can be calculated as  $([\text{ClO}_2^-]_0 - [\text{ClO}_2^-]_\infty)/[\text{S}_3\text{O}_6^{2-}]_0$ . In an excess of trithionate we also calculated SR to be defined as  $[\text{ClO}_2^-]_0/([\text{S}_3\text{O}_6^{2-}]_0 - [\text{S}_3\text{O}_6^{2-}]_\infty)$  from  $[\text{S}_3\text{O}_6^{2-}]_\infty$  determined by iodometry.<sup>19</sup> The result is illustrated in Figure 2, indicating that in trithionate excess, the SR is around 2, but as

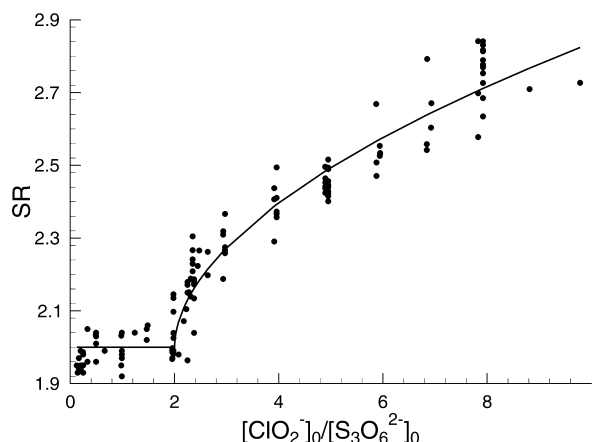
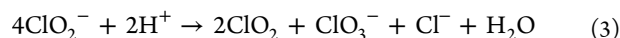
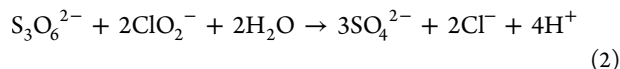


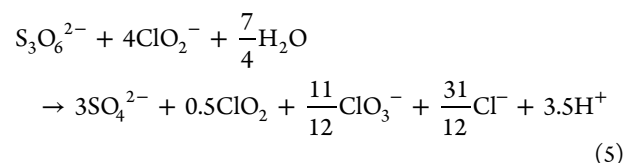
**Figure 2.** Experimental (dots) stoichiometric ratio (SR) as a function of initial concentration ratio of the reactants in buffered medium.

chlorite starts to be in excess, the SR continuously increases. It suggests that the actual stoichiometry of the reaction can be described by an appropriate linear combination of the following equations:



It evidently means that in principle a very high SR can be reached but in practice in buffered conditions we measured it not to be more than 3. However, in unbuffered conditions where  $[\text{H}^+]$  of the reacting solution can be varied by more than 2 orders of magnitude, this ratio may be shifted well above 3 as 1D-front propagating studies suggest (see later, Figure 4). As can be seen, the maximum of the front velocity is reached between 1:3 and 1:6 trithionate/chlorite ratios and a further increase in chlorite concentration results in a drastic decrease in the measured front velocity. At very high chlorite excess, the front even stops to propagate. The effect of trithionate concentration on the velocity of front reaction indicates saturation-like curves that almost levels off around around  $\text{SR} = 2$ , meaning that after reaching one of the limiting stoichiometries (eq 2) no sharp increase can be obtained by a further increase of  $\text{S}_3\text{O}_6^{2-}$  excess. Evidently, it means that chlorite becomes the limiting agent after reaching the limiting stoichiometry (eq 2) and the amount of autocatalyst cannot be increased further. Therefore, the slight increase in the measured front velocity is the sole consequence of the increasing reaction rate due to the trithionate concentration increase but not the combined effect of the amount of proton produced and the increasing reaction rate. Studies of the initially added hydroxide ion concentration against the velocity of front propagation show a linear dependence with an intercept, indicating a critical  $\text{OH}^-$  value above which no propagating front can be observed. These measurements suggest that the ratio of the amount of proton evolved in the reaction and the initial trithionate concentration should be around 3.5. Taking also into account that the maximum concentration of chlorine dioxide measured is approximately an order of magnitude lower than the consumed chlorite concentration during the course of the reaction and the maximum front velocity to be measured between the initial trithionate/chlorite ratio is between 1:3 and

1:6, we propose the following stoichiometry for simulating the concentration dependencies of the 1D-front propagation:



As can be seen, this stoichiometry can be set as the following linear combination of eqs 2–4:  $(5) = (2) + 0.25 \times (3) + 1/3 \times (4)$ .

**Initial Rate Studies.** Figure 3 shows results of the initial rate studies. As can be seen, log–log plots give perfect straight lines in the case of chlorite and hydrogen ion from which one can easily conclude that formal kinetic orders of chlorite and

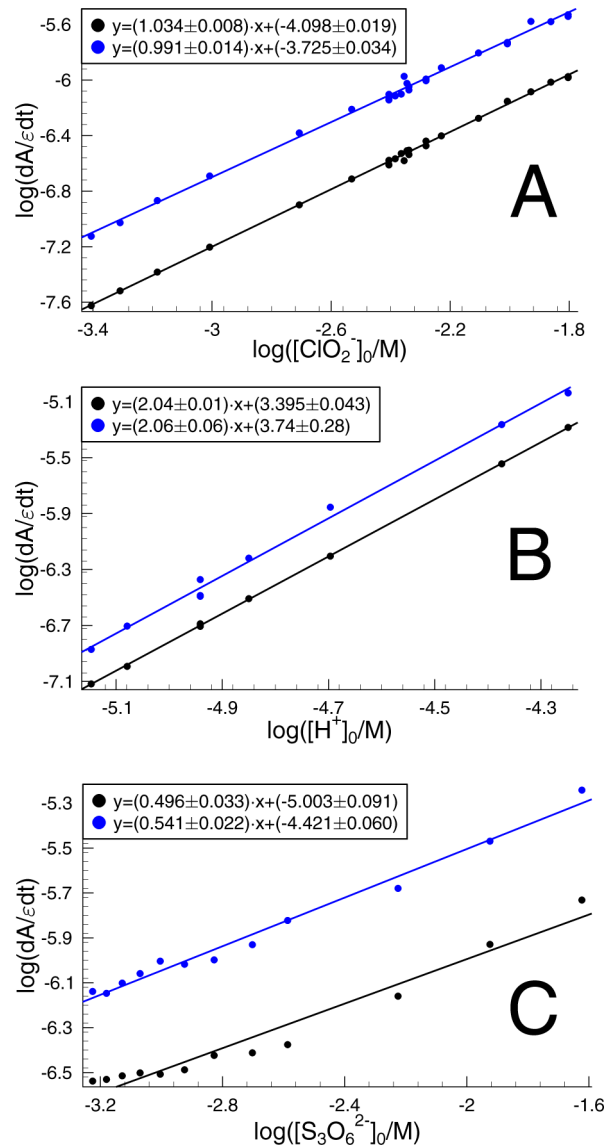


**Figure 3.** Initial rate studies in buffered medium. Conditions are as follows: (A)  $[\text{S}_3\text{O}_6^{2-}]_0 = 1.984 \text{ mM}$  and  $\text{pH} = 4.55$ ; (B)  $[\text{S}_3\text{O}_6^{2-}]_0 = 1.984 \text{ mM}$  and  $[\text{ClO}_2^-]_0 = 15.71 \text{ mM}$ ; (C)  $[\text{ClO}_2^-]_0 = 5.823 \text{ mM}$  and  $\text{pH} = 4.55$ . In the case of black and blue symbols and lines,  $\text{dA}/\text{dt}$  was calculated from absorbances measured at  $360 \text{ nm}$  ( $\epsilon = \epsilon_{\text{ClO}_2} = 1180 \text{ M}^{-1} \text{ cm}^{-1}$ ) and at  $290 \text{ nm}$  ( $\epsilon = \epsilon_{\text{ClO}_2} = 93.7 \text{ M}^{-1} \text{ cm}^{-1}$ ).

hydrogen are 1 and 2, respectively. A similar analysis for the kinetic order of trithionate gave approximately 0.5. Moreover, these statements are valid not only for the consumption of chlorite (absorbance measured at 290 nm) but also for the formation of chlorine dioxide (absorbance measured at 360 nm). However, a plot of the logarithm of the initial rate against the logarithm of initial trithionate concentrations indicates that the formal kinetic order of trithionate may vary as a function of trithionate concentration because the correlation is not perfectly linear. It suggests that the kinetics of the reaction even in the beginning stage of the reaction is very complex, so further study is required for complete elucidation of the mechanism of the chlorite–trithionate reaction. This fact does not seem to be surprising at all because in the case of chlorite–tetrathionate reaction the same phenomenon occurs in the case of the formal kinetic order of tetrathionate.<sup>23</sup> According to these data we conclude that the kinetics of the beginning stage of the reaction can be adequately described by the following rate equation:

$$-\frac{d[\text{ClO}_2^-]}{dt} = k_1[\text{S}_3\text{O}_6^{2-}]^{1/2}[\text{ClO}_2^-][\text{H}^+]^2 \quad (6)$$

where  $k_1$  was calculated to be  $(6.9 \pm 0.9) \times 10^6 \text{ M}^{-3.5} \text{ s}^{-1}$ .

**1D-Front Studies.** Figures 4–6 illustrate the front velocity against different reagent concentrations.

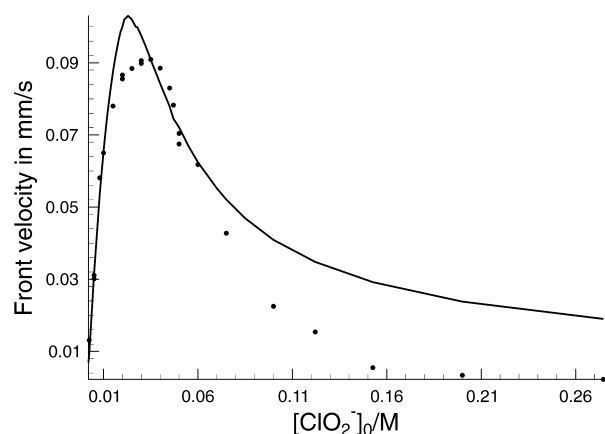


**Figure 4.** Experimental (dots) and calculated (solid line) front velocities against the initial concentration of the chlorite ion. Conditions are as follows:  $[\text{S}_3\text{O}_6^{2-}]_0 = 5.0 \text{ mM}$  and  $[\text{NaOH}]_0 = 1.0 \text{ mM}$ .

As can be seen, the front velocity is approximately proportional to the initially added hydroxide concentrations, a negative slope meaning that above a certain initial hydroxide concentration no front could be observed. This is well in accordance with the fact that, if autocatalytic production of  $\text{H}^+$  cannot compensate the bulk hydroxide concentration, the front cannot propagate. As mentioned, it also provided a good opportunity to establish the appropriate stoichiometry. The velocity of the front against the initial concentration of trithionate varied as a saturation-type curve, although at high concentrations we still observed some, but not a significant, increase in the velocity. According to the well-known Luther equation,<sup>24</sup> this observation can also be explained quite easily. The measured front velocity is proportional to the square root of the apparent rate coefficient of the autocatalytic pathway, which is further proportional to the square root of the

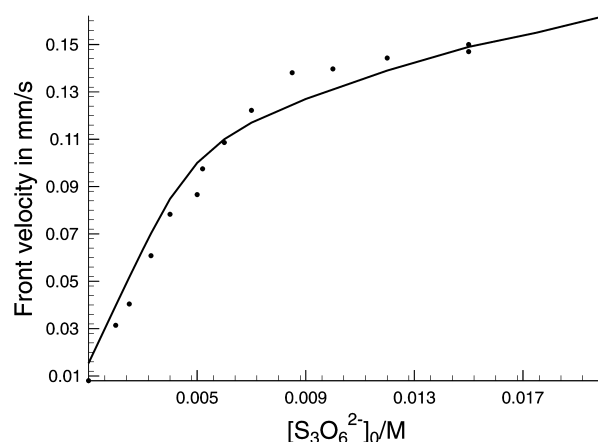


**Figure 5.** Experimental (dots) and calculated (solid line) front velocities against the initial concentration of the trithionate ion. Conditions are as follows:  $[\text{ClO}_2^-]_0 = 20.0 \text{ mM}$  and  $[\text{NaOH}]_0 = 1.0 \text{ mM}$ .

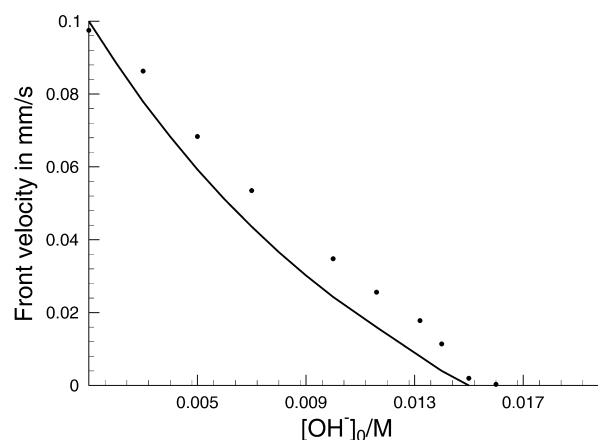


**Figure 6.** Experimental (dots) and calculated (solid line) front velocities against the initial concentration of the hydroxide ion. Conditions are as follows:  $[\text{ClO}_2^-]_0 = 20.0 \text{ mM}$  and  $[\text{S}_3\text{O}_6^{2-}]_0 = 5.0 \text{ mM}$ .

concentration of trithionate; hence the measured front velocity should be proportional to the fourth root of trithionate concentration. The most surprising result is seen when the effect of chlorite concentration on the velocity of the propagating front was studied. A clear maximum appeared between 1:3 and 1:6 initial concentration ratios of trithionate and chlorite. A further increase in the concentration of chlorite sharply decreases the velocity, and at a high excess of chlorite the front can even stop propagating. Certainly this phenomenon can only be explained by the fact that the concentration of free protons (autocatalyst of the system) decreases with increasing chlorite concentration. As we shall see, it will be the consequence of a fast and reversible protonation process of chlorite in acidic conditions. This fact was also enlightened in our previous paper,<sup>12</sup> but such a huge decelerating effect of chlorite on the front propagation was never measured.

**2D-Front Studies.** Table 1 contains the information of the 2D front propagation studies in a convection free system, where part of the autocatalyst was bound with different amounts of PPA immobilized in the gel.

As expected, within a rather wide concentration range of the reactants we could observe the fact that a linearly initiated front profile loses its stability to produce cellular structures. The key



**Table 1.** Concentration Space Indicating the Appearance of Linear Front Instability<sup>a</sup>

$[\text{ClO}_2^-]_0/\text{mM}$	$[\text{S}_2\text{O}_6^{2-}]_0/\text{mM}$	$[\text{OH}^-]_0/\text{mM}$	$[\text{PPA}]_0/\text{mM}$	instability
5.0–9.0	5.0	1.0	17.0	no
10.0–20.0	5.0	1.0	17.0	yes
30.0–40.0	5.0	1.0	17.0	no
11.0	1.0–3.0	1.0	17.0	no
11.0	6.0–16.0	1.0	17.0	yes
11.0	5.0	0.0–10.0	17.0	yes
11.0	5.0	15.0	17.0	no
11.0	5.0	1.0	7.0	no
11.0	5.0	1.0	10–17.0	yes
11.0	5.0	1.0	20.0–30.0	no

<sup>a</sup>The agarose and the congo red content were set to 0.08 and 0.6 wt %, respectively.

fact is that the flux of the autocatalyst (proton) should be in an appropriate range that results from the initial concentration of the reactants determining the rate of reaction, the amount of autocatalyst produced, and the initial concentrations of hydroxide ion and PPA that control the amount of autocatalyst. Figure 7 shows several snapshots, indicating the evolution of the linear front profile that eventually loses stability.

**Model for Front Propagation Studies.** Taking into account our earlier observations, the following simplified model is proposed for a description of the concentration dependence of the front velocity in the 1D system. The kinetics is determined by eq 5 along with its rate equation (eq 6), but this process must be augmented with the following rapidly established equilibria:



where the corresponding rate coefficients are as follows:  $k_2 = 10^{11} \text{ M}^{-1} \text{ s}^{-1}$ ,  $k_{-2}[\text{H}_2\text{O}] = 1.8 \times 10^{-3} \text{ M}^{-1} \text{ s}^{-1}$ ,  $k_3 = 10^{10} \text{ M}^{-1} \text{ s}^{-1}$ ,  $k_{-3} = 1.38 \times 10^8 \text{ s}^{-1}$ ,  $k_4 = 10^{10} \text{ M}^{-1} \text{ s}^{-1}$ , and  $k_{-4} = 5.75 \times 10^8 \text{ s}^{-1}$ . These rate coefficients were chosen in such a way that in each case the negative logarithm of the  $k_{-i}/k_i$  values should give the corresponding  $\text{p}K_w$  and  $\text{p}K_a$  values.<sup>25</sup> In the PDEs the diffusion constants of  $\text{H}^+$ ,  $\text{OH}^-$ ,  $\text{S}_2\text{O}_6^{2-}$ ,  $\text{ClO}_2^-$ ,  $\text{HClO}_2$ ,  $\text{HSO}_4^-$ , and  $\text{SO}_4^{2-}$  were set to  $1.4 \times 10^{-4}$ ,  $8 \times 10^{-5}$ ,  $8.4 \times 10^{-6}$ ,  $1.3 \times 10^{-5}$ ,  $1.3 \times 10^{-5}$ ,  $1.1 \times 10^{-5}$ , and  $1.1 \times 10^{-5}$ , respectively. The diffusion constants of hydrogen ion, hydroxide ion, and sulfate were directly taken from ref 26. The other values were calculated from  $D_{\text{SO}_4^{2-}}$  with the help of the approximate equation  $D_i M_i^{1/2} = \text{constant}$ , where  $M_i$  is the ionic weight.

To simulate the 1D-front propagation, we first used the  $k_1 = 6.9 \times 10^6 \text{ M}^{-3.5} \text{ s}^{-1}$  value determined in a buffered medium but found that the calculated 1D-front propagating values approximately 8 times higher than the measured ones. However, decreasing the rate coefficient of eq 5 to  $k_1 = 1.02 \times 10^5 \text{ M}^{-3.5} \text{ s}^{-1}$  indicates a sound agreement between the measured and calculated data shown in Figures 4–6. A straightforward question, however, immediately arises about the difference between the measured and used  $k_1$  values. Certainly in the case of the kinetic measurement the ionic strength was set to 0.5 M but in the case of front propagation

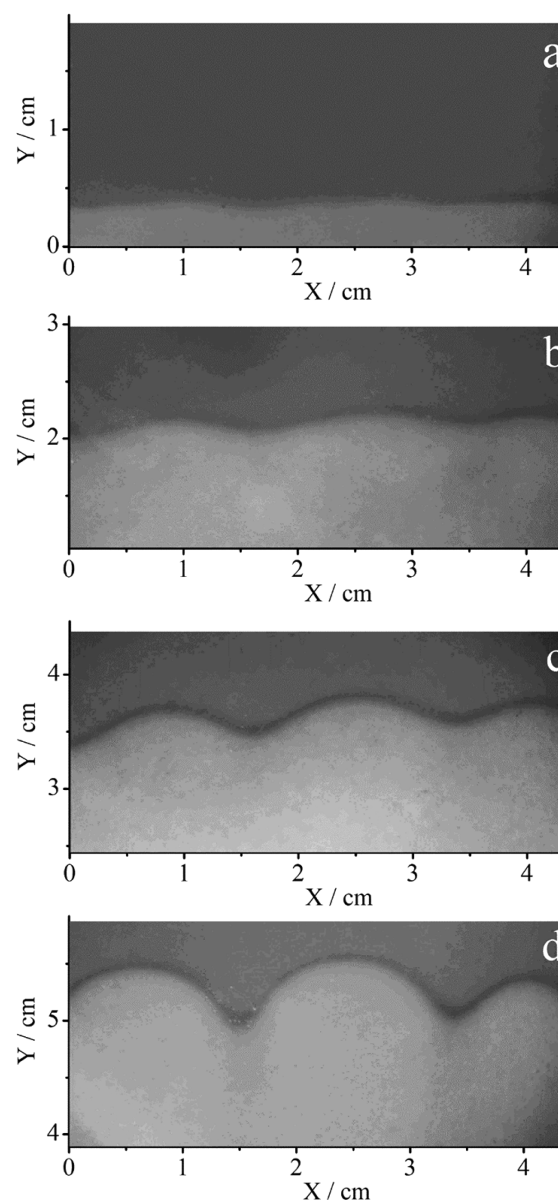


**Figure 7.** Snapshots indicating cellular structures at different time points. Conditions:  $[\text{ClO}_2^-]_0 = 11.0 \text{ mM}$ ,  $[\text{S}_2\text{O}_6^{2-}]_0 = 5.0 \text{ mM}$ ,  $[\text{OH}^-]_0 = 1.0 \text{ mM}$ ,  $[\text{PPA}]_0 = 17.0 \text{ mM}$ . The images were taken 1 h (a), 8 h (b), 16 h (c), and 24 h (d) after initiation, respectively.

studies the ionic strength was maintained by the concentration of the reactants; hence it was much lower in the latter case. Taking into account that a positive salt effect is expected in the case of increasing ionic strength between two like charge ions, part (but not all) of this huge difference (69 times) may be explained. The other reason would be the application of acetic acid/acetate buffer if buffer assistance were involved in the kinetics of the title reaction. Figure 8 shows the effect of the concentration of buffer components on the initial rate at constant ionic strength.

As can be seen, the initial rate marginally increases with increasing buffer concentration; therefore, the special catalytic effect of buffers should also be considered in the title reaction. Moreover, not only the initial rate but also the shape of the absorbance–time profiles varies significantly. Hence we suggest that the combined effect of the ionic strength and special buffer catalysis should account for the deviation in  $k_1$  determined

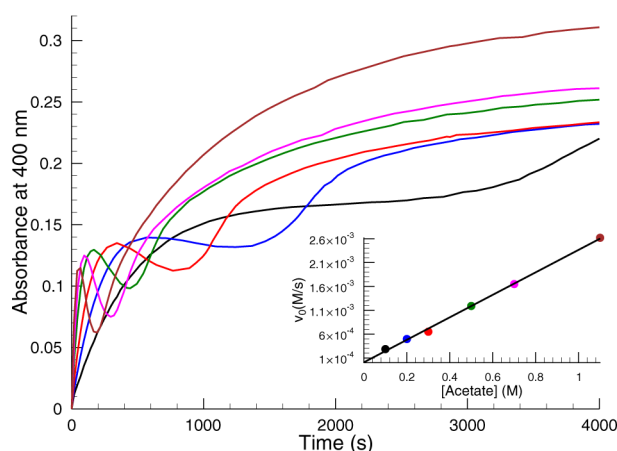


**Figure 8.** Experimental absorbance–time profiles in the chlorite–trithionate reaction at an ionic strength  $I = 1.5$  M adjusted by the necessary amount of sodium perchlorate and at  $[\text{HOAc}]/[\text{OAc}^-] = 1$  with changing buffer component concentrations. Conditions are as follows:  $[\text{S}_3\text{O}_6^{2-}]_0 = 3.0$  mM;  $[\text{ClO}_2^-]_0 = 12.0$  mM,  $[\text{OAc}^-]_0/M = 0.1$  (black); 0.2 (blue); 0.3 (red); 0.5 (green); 0.7 (magenta); 1.1 (brown). The inset shows the calculated initial rates (dots) with changing acetate concentration. The color of dots means that the given value was determined from the absorbance–time profile having the same color. Parameters of the fitted straight line is slope =  $(2.36 \pm 0.25) \times 10^{-3}$  and intercept =  $(8.49 \pm 2.53) \times 10^{-5}$ .

experimentally but used in the 1D simulation studies. To support further this idea, from the intercept of the straight line as a plot of initial rate against the acetate concentration (see the inset of Figure 8), one can easily calculate  $k_1 = (1.38 \pm 0.41) \times 10^5 \text{ M}^{-3.5} \text{ s}^{-1}$ , which is in very sound agreement with the value of  $k_1$  used in the simulations.

It should also be noted that although the proposed model accounts well for the most important characteristics of the measured front velocities still some systematic deviations could be encountered, especially at high chlorite concentrations. As already noted, our model is working with a strict stoichiometry but kinetic measurements suggest that at a high excess of chlorite the SR increases. Therefore, one possible improvement of our model is to account well for the shift in the stoichiometry as a function of the trithionate/chlorite ratio. If this shift is accompanied by less proton production, then the simulated front velocities should also decrease in harmony with our experiments. Because a large excess of chlorite eventually shifts the stoichiometry of the reaction toward chlorine dioxide production (eq 3), it evidently decreases the amount of proton produced; hence, the simulated front velocity is expected to decrease. Another possible improvement of the present model is to account precisely for the formal kinetic order of trithionate that also changes slightly (Figure 3C). These improvements, however, would require further detailed kinetic studies that will be conducted in our lab in the near future. It should be mentioned, however, that these improvements would definitely complicate the present model and increase significantly the time of the calculation processes required, especially in 2D studies, and therefore, they may bring into question an easier applicability.

## CONCLUSION

We have demonstrated, in this manuscript, that as a tool the chlorite–trithionate reaction is a better alternative possibility to study nonlinear dynamical phenomena in connection with front

propagation over the most widely used chlorite–tetrathionate system. A simple kinetic model is proposed that works semiquantitatively well to simulate the seemingly unusual concentration dependencies of the 1D front propagation as a function of initial chlorite concentration. The main advantage of this system over the CT reaction is that the substrate (trithionate) is much more stable in alkaline conditions besides the fact that it also has all the most important kinetic features that made the original CT reaction attractive for studying spatiotemporal structures.

## AUTHOR INFORMATION

### Corresponding Authors

\*Q. Gao: e-mail, gaoqy@cumt.edu.cn.

\*A. K. Horváth: e-mail, horvatha@gamma.ttk.pte.hu.

### Notes

The authors declare no competing financial interest.

## ACKNOWLEDGMENTS

This work was supported by Grants 21073232 and 51221462 from the National Natural Science Foundation of China, the Fundamental Research Funds for the Central Universities (No. 2013XK05) and PAPD. Some experiments of 1D front propagation studies done by Ms. Tamara Papp are also acknowledged. The authors are also grateful to the financial support of the Chinese-Hungarian Cooperative Grant K-TÉT-12-CN-1-2012-0030 and SROP No.: 4.2.2./A-11/1/KONV-2012-0065.

## REFERENCES

- (1) Gauffre, F.; Labrot, V.; Boissonade, J.; Kepper, P. D.; Dulos, E. Reaction-Diffusion Patterns of the Chlorite-Tetrathionate System in a Conical Geometry. *J. Phys. Chem. A* **2003**, *107*, 4452–4456.
- (2) Horváth, D.; Tóth, A. Diffusion-Driven Front Instabilities in the Chlorite–Tetrathionate Reaction. *J. Chem. Phys.* **1998**, *108*, 1447–1451.
- (3) Fuentes, M.; Kuperman, M. N.; Kepper, P. D. Propagation and Interaction of Cellular Fronts in a Closed System. *J. Phys. Chem. A* **2001**, *105*, 6769–6774.
- (4) Vasquez, D. A.; Wit, A. D. Dispersion Relations for the Convective Instability of an Acidity Front in Hele-Shaw Cells. *J. Chem. Phys.* **2004**, *121*, 935–941.
- (5) Virányi, Z.; Horváth, D.; Tóth, A. Migration-Driven Instability in the Chlorite-Tetrathionate Reaction. *J. Phys. Chem. A* **2006**, *110*, 3614–3618.
- (6) Lima, D.; D’Onofrio, A.; Wit, A. D. Nonlinear Fingering Dynamics of Reaction-Diffusion Acidity Fronts: Self-Similar Scaling and Influence of Differential Diffusion. *J. Chem. Phys.* **2006**, *124*, 014509.
- (7) Rica, T.; Horváth, D.; Tóth, A. Viscosity-Change-Induced Density Fingering in Polyelectrolytes. *J. Phys. Chem. B* **2008**, *112*, 14593–14596.
- (8) Boissonade, J.; Dulos, E.; Gauffre, F.; Kuperman, M. N.; Kepper, P. D. Spatial Bistability and Waves in a Reaction with Acid Autocatalysis. *Faraday Discuss.* **2002**, *120*, 353–361.
- (9) Szalai, I.; Gauffre, F.; Labrot, V.; Boissonade, J.; Kepper, P. D. Spatial Bistability in a pH Autocatalytic System: From Long to Short Range Activation. *J. Phys. Chem. A* **2005**, *109*, 7843–7849.
- (10) Tóth, A.; Horváth, D.; Siska, A. Velocity of Propagation in Reaction-Diffusion Fronts of the Chlorite–Tetrathionate Reaction. *J. Chem. Soc., Faraday Trans.* **1997**, *93*, 73–76.
- (11) Horváth, A. K. A Three-Variable Model for the Explanation of the “Supercatalytic” Effect of Hydrogen Ion in the Chlorite-Tetrathionate Reaction. *J. Phys. Chem. A* **2005**, *109*, 5124–5128.
- (12) Peintler, G.; Csekő, G.; Petz, A.; Horváth, A. K. An Improved Chemical Model for the Quantitative Description of the Front

Propagation in the Tetrathionate-Chlorite Reaction. *Phys. Chem. Chem. Phys.* **2010**, *12*, 2356–2364.

(13) Gutman, A. Ueber die Einwirkung von Cyankalium auf Natrium-Tetrathionate und -Dithionat. *Ber. Dtsch. Chem. Ges.* **1906**, *39*, 509–513.

(14) Riesenfeld, E. H. Über die Bildung und Zersetzung von Polythionaten. *Z. Anorg. Allg. Chem.* **1924**, *141*, 109–110.

(15) Zhang, H.; Dreisinger, D. B. The Kinetics for the Decomposition of Tetrathionate in Alkaline Solutions. *Hydro-metallurgy* **2002**, *66*, 59–65.

(16) Varga, D.; Horváth, A. K. Kinetics and Mechanism of the Decomposition of Tetrathionate Ion In Alkaline Medium. *Inorg. Chem.* **2007**, *46*, 7654–7661.

(17) Rolia, E.; Chakrabarti, C. L. Kinetics of Decomposition of Tetrathionate, Trithionate and Thiosulfate in Alkaline Media. *Environ. Sci. Technol.* **1982**, *16*, 852–857.

(18) Pan, C. W.; Wang, W.; Horváth, A. K.; Xie, J.; Lu, Y.; Wang, Z.; Ji, C.; Gao, Q. Kinetics and Mechanism of Alkaline Decomposition of the Pentathionate Ion by the Simultaneous Tracking of Different Sulfur Species by High-Performance Liquid Chromatography. *Inorg. Chem.* **2011**, *50*, 9670–9677.

(19) Csekő, G.; Horváth, A. K. Non-Triiodide Based Autoinhibition by Iodide Ion in the Trithionate–Iodine Reaction. *J. Phys. Chem. A* **2010**, *114*, 6521–6526.

(20) Liu, H.; Pojman, J. A.; Zhao, Y.; Pan, C. W.; Zheng, J.; Yuan, L.; Horváth, A. K.; Gao, Q. Pattern Formation in the Iodate-Sulfite-Thiosulfate Reaction-Diffusion System. *Phys. Chem. Chem. Phys.* **2012**, *14*, 131–137.

(21) Lambert, J. D., Ed. *Numerical Methods for Ordinary Differential Systems. The Initial Value Problem*, 1st ed.; John Wiley & Sons: Chichester, U.K., 1991.

(22) Csekő, G.; Horváth, A. K. Kinetics and Mechanism of the Chlorine Dioxide–Trithionate Reaction. *J. Phys. Chem. A* **2012**, *116*, 2911–2919.

(23) Horváth, A. K.; Nagypál, I.; Peintler, G.; Epstein, I. R. Autocatalysis and Self-Inhibition: Coupled Kinetic Phenomena in the Chlorite–Tetrathionate Reaction. *J. Am. Chem. Soc.* **2004**, *114*, 6246–6247.

(24) Luther, R. Raumliche Fortpanzung Chemischer Reaktionen. *Z. Elektrochem.* **1906**, *12*, 596–600.

(25) IUPAC Stability Constant Database v3.04, [www.acadsoft.co.uk](http://www.acadsoft.co.uk).

(26) Weast, R. C., Ed. *Handbook of Chemistry and Physics*, 64th ed.; CRC Press: Boca Raton, FL, USA, 1983.